Iranian Journal of Veterinary Research, Shiraz University, Vol. 10, No. 1, Ser. No. 26, 2009

Short Paper

Magnetic resonance imaging of feline eye

Vosough, D.[1*]; Shojaei, B.[2] and Molazem, M.[3]

[1]Department of Clinical Sciences, Faculty of Veterinary Medicine, Shahid Bahonar University of Kerman, Kerman, Iran; [2]Department of Basic Sciences, Faculty of Veterinary Medicine, Shahid Bahonar University of Kerman, Kerman, Iran; [3]Ph.D. Student in Radiology, Department of Clinical Sciences, Faculty of Veterinary Medicine, University of Tehran, Tehran, Iran

[*]**Correspondence:** D. Vosough, Department of Clinical Sciences, Faculty of Veterinary Medicine, Shahid Bahonar University of Kerman, Kerman, Iran. E-mail: dvosugh@yahoo.com

(Received 12 Feb 2008; revised version 20 Oct 2008; accepted 14 Dec 2008)

Summary

The purpose of this study was to investigate magnetic resonance imaging (MRI) of the normal feline eye and optic nerves using T_1-weighted and T_2-weighted images. A total of 6 healthy female domestic short hair cats age 2-2.5 years and weighing 3.2 ± 0.4 kg were selected. Magnetic resonance imaging data were collected using GEMSOW (Philips) at a magnetic field strength of 1.5 T. Dorsal, sagittal, and transverse plane images were obtained from left and right eyes. Intraocular structures of the cats visible on T_1-weighted and T_2-weighted images include cornea, anterior chamber, posterior chamber, lens, iris, sclera, and chiasma. Cornea was well detected in T_1-weighted, the iris in T_2-weighted and chiasma was well detected in T_2-weighted in dorsal plane. Measurements of the visible structures on T_1-weighted and T_2-weighted images did not show any significant difference between the left and right eyes ($P>0.05$). MRI provides excellent anatomical detail of the feline eye and optic nerve due to its superior soft tissue contrast and its multiplanar and multislice imaging capability.

Key words: MRI, Eye, Feline, Optic nerve

Introduction

Despite almost unrestricted access to the eye and orbit, additional diagnostic imaging is frequently required to diagnose a variety of ocular, orbital, and optic nerve conditions in veterinary medicine. Contrast radiography, ultrasonography, and computerized tomography have been reported as useful diagnostic aids in a variety of veterinary ophthalmic disorders. Since the eye is made of different soft tissues and liquids, there must be a good signal production by magnetic resonance imaging (MRI) (Bruce *et al*., 1993). Sometimes it is also difficult to detect inner parts of the eye because of cataract or kratitis. Various systemic diseases like fungal infections, lupus, and vitamin E deficiency can involve optical nerve which is not detectable by conventional ultrasonography or ophthalmoscopy (Nyland and Matton, 2002). In this study, sagittal, transverse, and dorsal MRI planes of intra-orbital structures such as cornea, anterior and posterior chambers, lens axis, iris, and post-orbital structures such as optic nerve and the best plane for each individual structure in cats are introduced. T_1-weighted and T_2-weighted signal intensities were also compared together. All the orbital structures of the cats were investigated for their hypointensity, hyperintensity, homogeneity, and heterogeneity. The sizes of the orbital structures were compared in the left and right eyes.

Materials and Methods

A total of 6 healthy female domestic short hair cats weighing 3.2 ± 0.4 kg and age 2-2.5 years were selected. They were normal on clinical and paraclinical examinations. Magnetic resonance imaging data were

collected using GEMSOW (Philips) at a magnetic field strength of 1.5 tesla. Dorsal, sagittal, and transverse plane images were obtained from left and right eyes. A 13 cm diameter RF coil was used. All cases underwent general anesthesia by ketamin (20 mg/kg) and diazepam (0.02 mg/kg) and positioned in ventral recumbency with their head inside the RF coil.

The field of view (FOV) was selected as the smallest amount possible to only reduce the wrap-around artifacts and not reducing signal noise ratio (SNR). Dorsal plane images were obtained using T_2-weighted (TE = 97 msec, TR = 42000 msec, matrix = 256 × 192 and FOV = 17.17) to measure the optic nerve (Fig. 1). Sagittal plane images were obtained using T_2-weighted (TE = 88.3 msec, TR = 4000 msec, matrix = 320 × 256 and FOV = 16.16) and T_1-weighted (TE = 36.8 msec, TR = 500 msec, matrix = 256.224 and FOV = 16.16) to measure the orbital structures (Figs. 2 and 3).

Results

Intraocular structures of the cats visible on T_1-weighted and T_2-weighted images include cornea, anterior chamber, posterior chamber, lens, iris, sclera, and chiasma. Cornea was well detected in T_1-weighted and the iris in T_2-weighted (Fig. 3).

The image signal intensity of the aqueous and vitreous humor were low on T_1-weighted and high on T_2-weighted images when compared to brain tissue. Sclera had low signal intensity on T_1-weighted and T_2-weighted images.

Aqueous, vitreous humor, and the lens were homogenous on T_1-weighted and T_2-weighted images and the iris was heterogeneous. Optic nerve had a moderately high signal on T_1-weighted in comparison with vitreous humor, and it had moderately low signal comparison with vitreous humor and was more visible on T_2-

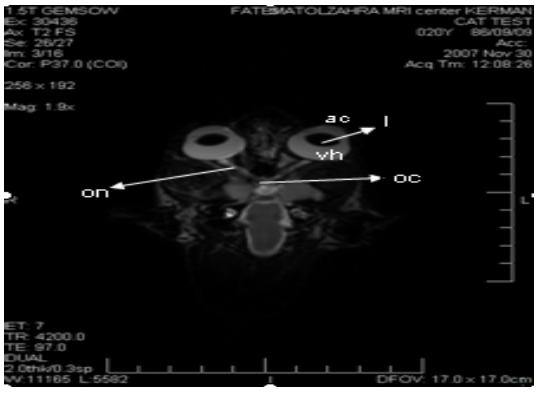

Fig. 1: T_2-weighted magnetic resonance dorsal images through the brain, eyes and orbit of a normal cat (TE = 97 msec, TR = 42000 msec). Normal structures are identified: ac = anterior chamber; l = lense; on = optic nerve; oc = optic chiasma; vh = vitreous humor. In this plane the optic nerve was measured

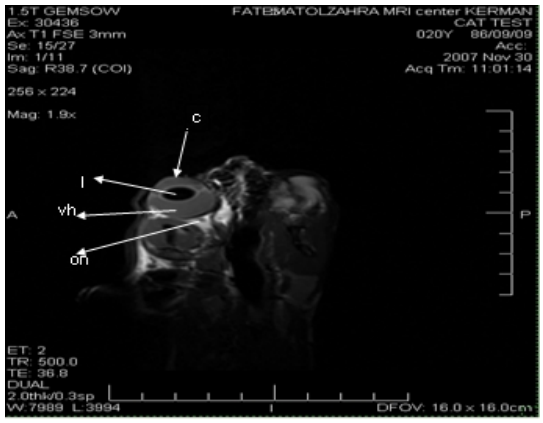

Fig. 2: T_1-weighted magnetic resonance sagittal images through the brain, right eye and orbit of a normal cat (TE = 36.8 msec, TR = 500 msec). Normal structures are identified: c = cornea; l = lense; on = optic nerve; vh = vitreous humor. In this plane lense, cornea and vitreous humor were measured

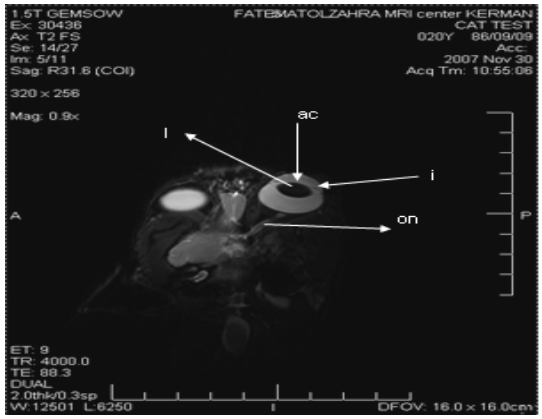

Fig. 3: T_2-weighted magnetic resonance sagittal images through the brain, right eye and orbit of a normal cat (TE = 88.3 msec, TR = 4000 msec). Normal structures are identified: i = iris; l = lense; ac = anterior chamber; on = optic nerve. In this plane anterior chamber, lense and vitreous humor were measured. Iris was well detected in this plane

weighted images in comparison with T_1-weighted images. Chiasma optic was observed with better quality in T_2-weighted in dorsal plane (Figs. 1, 2 and 3).

Measurements of the visible structures on T_1-weighted and T_2-weighted images did not show any significant difference between the left and right eyes ($P>0.05$; Table 1). Optical nerve size was measured in axial plane and anterior chamber, lens, vitreous humor, and orbital axis on sagittal plane (Figs. 1, 2 and 3).

Table 1: Mean measurement (mm) and standard deviation (SD) of the internal structure and optic nerve of the right and left eyes in six female domestic short hair cats

Parameter	Right eye		Left eye	
	Mean	SD	Mean	SD
Lens long axis	0.501	0.1	0.503	0.12
Cornea	0.05	0.01	0.053	0.02
Anterior chamber	0.395	0.12	0.398	0.13
Vitreous body	0.701	0.13	0.703	0.11
Optic nerve	0.169	0.09	0.170	0.085
Long axis	1.7	0.1	1.73	0.14

Discussion

This study confirms that magnetic resonance imaging is useful in investigating orbital structures. There is a potent high contrast from great amount of fat surrounding the anatomical structures of the cat's eyes. This fat accumulation is a good tool to differentiate soft tissues (muscles and optical nerve) from hard tissues (bones). MRI can demonstrate most of pathological processes which destroyed bony structures (e.g. tumors). MRI is considered as an excellent imaging modality for a variety of human ophthalmic conditions, because it provides high soft tissue contrast, multiplanar imaging capabilities, precise anatomical detail, flexible image contrast, and tissue pathology-specific images. MRI studies of the human eye, orbit, and optic nerves have shown not only the extent of pathological conditions, but also specific tumor images based on anatomical location and signal intensity. For example melanomas appear bright (high signal intensity) on T_1-weighted and dark (low signal intensity) on T_2-weighted images (Felix *et al*., 1985). Sarcomas, however, are characterized by low signal images on T_1-weighted and high signal intensity on T_2-weighted images (Peyster *et al*., 1985). Volumetry and distribution of melanomas are also possible by this technique to help pre-operation planning, precluded successful surgical removal, and therapeutic response to radiation (Marx *et al*., 1990; Sullivan and Harms, 1996). Garcia *et al*. (2005) measured the optical nerve diameter by MRI and three-dimensional ultrasonography in human. Whereas, there are a few reports in veterinary practice using MRI in animal eye examinations. For instance, different orbital structures were investigated in rabbit (Cecker *et al*., 1991) and cow in T_1- and T_2-weighted images (William *et al*., 1990). Bruce *et al*. (1993) reported orbital melanoma and meningioma in cats by using MRI; they also used gadolinium-DTPA to assess the eye in proton density-weighted scanning.

In this study the measurement of the internal structure of the eye and optic nerve were the same as study done by Evans and Christensen (2002).

In conclusion, our results demonstrate the great potential of MRI for imaging ocular, orbital, and optic nerve lesions in the cats. Lack of ionizing radiation and direct multiplanar, multislice imaging capabilities are specific advantages of MRI in regard to the ocular structures. The disadvantages of MRI include its limited availability to the veterinarian, and the requirement for general anesthesia to limit motion artifacts in the image. Metal objects in the patient's body are also a contraindication in the use of MRI.

References

Bruce, HG; Wendy, AS; Rheal, AT and Michael, D (1993). Magnetic resonance imaging of the canine and feline eye. Can. Vet. J., 34: 418-422.

Cecker, TL; Karino, K; Kador, PF and Balaben, RS (1991). Magnetic resonance imaging of the rabbit eye. Invest. Ophthalmol. Vis. Sci., 32: 3109-3113.

Evans, HE and Christensen, GC (2002). *Miler's anatomy of the dog*. 2nd Edn., W. B. Saunders Co., PP: 1073-1076.

Felix, R; Scharner, W and Laniado, M (1985).

Brain tumours: MR imaging with gadolinium-DTPA. Radiology. 156: 681-688.

Garcia, JP; Garcia, PM; Rosen, RB and Finger, PT (2005). Optic nerve measurements by 3D ultrasound-based coronal C-Scan imaging. Ophthalmic Surg. Lasers Imaging. 36: 142-146.

Marx, HF; Colletti, PM; Raval, JK; Boswell, WD and Zee, CH (1990). Magnetic resonance imaging features in melanoma. Magn. Reson. Imaging. 8: 223-229.

Nyland, TG and Matton, JS (2002). *Small animal diagnostic ultrasound*. 2nd Edn., W. B. Saunders Co., PP: 306-322.

Peyster, RG; Augsburg, JJ; Shields, JA; Herchey, BL and Eagle Rehashing, ME (1985). Intraocular tumours: evaluation with MR imaging. Radiology. 156: 669-674.

Sullivan, JA and Harms, SE (1996). Surface-coil MR imaging of orbital neoplasm. Am. J. Neurol., 7: 29-34.

William, TR; Perry, BC and Koenig, JL (1990). Magnetic resonance imaging of bovine ocular tissue. Ophthalmic Res., 22: 89-94.